Heterogeneous & Homogeneous & Bio- & Nano-

CHEMCATCHEM

CATALYSIS

Accepted Article

Title: Fe-based complexes as styrene aziridination catalysts: ligand substitution tunes catalyst activity

Authors: Guillaume Coin, Ranjan Patra, Martin Clémancey, Patrick Dubourdeaux, Jacques Pécaut, Colette Lebrun, Ludovic Castro, Pascale Maldivi, Sylvie Chardon-Noblat, and Jean-Marc Latour

To be cited as: *ChemCatChem* 10.1002/cctc.201901211

Link to VoR: http://dx.doi.org/10.1002/cctc.201901211

A Journal of

ChemPubSoc Europe

WILEY-VCH

www.chemcatchem.org

WILEY-VCH

COMMUNICATION

Fe-based complexes as styrene aziridination catalysts: ligand substitution tunes catalyst activity

Guillaume Coin,[ab$&] Ranjan Patra,[acd&] Martin Clémancey,[a] Patrick Dubourdeaux,[a] Jacques Pécaut,[c] Colette Lebrun,[c] Ludovic Castro,[c] Pascale Maldivi,[c] Sylvie Chardon-Noblat,[b*] Jean-Marc Latour[a*]

Dedication ((optional))

Abstract: As part of our effort to improve our understanding of aziridination mechanism, we used tetra substitution of a diphenol ligand to modify the redox properties of corresponding Fe complexes. This allowed us to confirm that aziridination catalysis by Fe-based complexes is governed by electron affinity of the active species and further show that it correlates with the Fe^{III}/Fe^{II} redox potential.

Nitrene transfer reactions have emerged in the past decade as a general and efficient tool to synthesize various kinds of amines,[1] the nitrene being generated by metal decomposition of a precursor. A strong research effort is currently devoted to replacing second row metal-based (i.e. Rh[2]) catalysts by more ecofriendly first row transition metals,[3–6] and in particular iron.[7] A favored way to achieving this goal aims at elucidating mechanistic aspects of the reaction by in-depth integrated experimental and calculational studies. This was done in particular for sulfimidation[8,9] and amination[8–11] by a few Fe reference systems. However, a comparable understanding has not yet been attained for aziridination[12,13] in spite of recent such studies.[14–16] Aziridines are interesting not only as pharmaceutical targets but also as useful synthetic intermediates through easy opening of their three-membered ring. Many different kinds of Fe aziridination catalysts have been developed over more than three decades. These include heme-[17,18] and dipyrromethene-based[19] catalysts, linear[15] and macrocyclic[20] carbene complexes, polyamine[21–24] systems and even Fe salts.[25] Basic mechanistic features were studied thanks to a few Hammett correlations. They revealed quite diverse behaviors dominated by radical delocalization[19] or instead governed by polarity effects, the active species being either electrophilic[21,24] or nucleophilic.[15]

We reported recently a combined experimental and computational mechanistic study of aziridination using Fe phenolate catalysts. The most active catalyst studied was the dinuclear $Fe^{III}Fe^{II}$ compound **(1)**[26,27] that was compared to the mono Fe^{II} complex $\mathbf{L^{Cl}Fe^{II}(MeCN)_2}$ (Scheme 1). These kinds of mono Fe complexes were known for their versatility and easy tunability and had been previously used for various catalytic reactions.[28–36] Our study disclosed that, for **(1)** and $\mathbf{L^{Cl}Fe^{II}(MeCN)_2}$, the aziridination reaction (Scheme 2) is governed essentially by the electron affinity (EA) of the high-valent Fe^{IV} imido active species which is best described as $\mathbf{L^{Cl}Fe^{III}\text{-}{}^{\bullet}NTs}$.[14] EA manifests in promoting in the transition state a partial electron transfer from the olefin to the Fe-bound tosylnitrene, a feature consistent with the moderately negative slope of Hammett-like correlations.

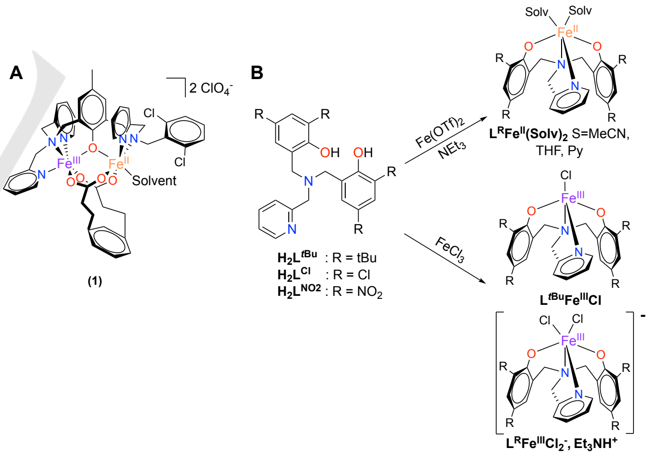

Scheme 1. Schematic representation of diphenol ligands and complexes.

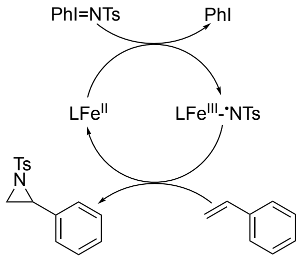

Scheme 2. Fe^{II}-catalyzed aziridine formation.

[a] Dr. G. Coin, Dr. R. Patra, Dr. M. Clémancey, Mr. P. Dubourdeaux, Dr. J.-M. Latour
Univ. Grenoble Alpes, CEA, CNRS, IRIG, LCBM, 38000 Grenoble, France,
E-mail: jean-marc.latour@cea.fr
[b] Dr. G. Coin, Dr. S. Chardon-Noblat
Univ. Grenoble Alpes, CEA, CNRS, DCM, 38000 Grenoble, France
E-mail: sylvie.chardon@univ.grenoble-alpes.fr
[c] Dr. R. Patra, Dr. J. Pécaut, Mrs. C. Lebrun, Dr. L. Castro, Dr. P. Maldivi
Univ. Grenoble Alpes, CEA, CNRS, IRIG, DIESE, SYMMES, 38000 Grenoble, France
[d] Dr. R. Patra
Amity Institute of Click Chemistry Research & Studies (AICCRS)
Amity University, Sector-125, Noida, India
$ Present address: Department of Chemistry and Applied Biosciences, ETH Zürich, 8093 Zürich, Switzerland
& These authors contributed equally

Supporting information for this article is given via a link at the end of the document.((Please delete this text if not appropriate))

However the mechanistic variability revealed recently[15,24] prompted us to investigate further the above phenolate system. Indeed, we reasoned that variation of the ligand substitution should affect the electron affinity of the active complex and thereby its catalytic efficiency. We have thus extended our series of ferrous $\mathbf{L^{R}Fe^{II}(Solv)_{x}}$ complexes (R = *t*Bu, Cl, NO_2; x = 1 or 2; Solv = CH_3CN, thf or pyridine (Scheme 1) to ligands with a strongly electron donating *t*Bu ($\mathbf{H_2L^{\mathit{t}Bu}}$) and a strongly electron withdrawing NO_2 ($\mathbf{H_2L^{NO2}}$). This tetranitro ligand had never been synthesized before.

The aziridination catalytic efficiencies were assessed and gratifyingly, aziridination yields paralleled EAs of the purported active species thus consolidating our initial conclusion. To further investigate the ligand influence we prepared chlorido mono ferric $\mathbf{L^{\mathit{t}Bu}Fe^{III}Cl}$ and $\mathbf{L^{R}Fe^{III}Cl_2(Et_3NH)}$ complexes (R = Cl or NO_2, Scheme 1) and measured by cyclic voltammetry (CV) their Fe^{III}/Fe^{II} reduction potentials. We found that aziridination yields correlate also with these potentials. This strengthens the link between aziridination activity and electronic properties and allows an estimation of the catalytic ability of a given system.

The *t*Bu- and Cl-substituted ligands (Scheme 1) are synthesized through a classical Mannich condensation, which is not possible for $\mathbf{H_2L^{NO2}}$. We thus devised a three-step synthetic route from 3,5-dinitrosalicylaldehyde (Scheme S1) allowing one to obtain it as a yellow powder in 80 % overall yield. The increased acidity of $\mathbf{H_2L^{NO2}}$, brought about by the four nitro groups, was evidenced by its X-ray structure (Figure S7) given that it crystallized as $\mathbf{[L^{NO2}H(H_2O)][(iPr)_2EtNH]}$ where the two phenols are deprotonated and participate in a H-bond network.

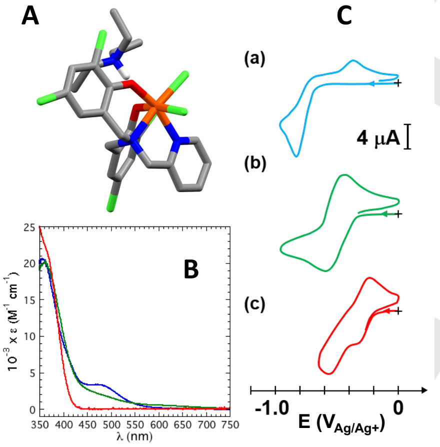

Figure 1. (A) X-ray structure of the complex $\mathbf{[L^{Cl}Fe^{III}Cl_2](Et_3NH)}$. For the sake of clarity, hydrogen atoms are not shown, except that of the ammonium countercation. (B) UV-vis. spectra of the ligand $\mathbf{H_2L_{NO2}}$ (red line), $\mathbf{[L^{NO2}Fe^{III}Cl_2](Et_3NH)}$ (blue line) and $\mathbf{L^{NO2}Fe^{II}(Py)_2}$ (green line). (C) Cyclic voltammograms of 1 mM $\mathbf{L^{\mathit{t}Bu}Fe^{III}Cl}$ (a) and $\mathbf{[L^{R}Fe^{III}Cl_2]^-}$ R = Cl (b) and NO_2 (c) in CH_3CN + 0.1 M TBAP (v = 100 mV s^{-1} on VC electrode diam. 3 mm, reference electrode Ag/Ag(NO_3) 0.01 M).

$\mathbf{L^{R}Fe^{II}(Solv)_{x}}$ and $\mathbf{L^{R}Fe^{III}}$ chlorido complexes (Scheme 1) were prepared according to published procedures by reaction of $\mathbf{H_2L^{R}}$ ligand with $Fe(OTf)_2$[14] or $FeCl_3$[31] in presence of triethylamine and were characterized by usual methods (see below and SI). The X-ray structure of the ferric complex $\mathbf{[L^{Cl}Fe^{III}Cl_2](Et_3NH)}$ was determined (Figure 1A). It shows that the Fe^{III} ion is hexacoordinated by the $\mathbf{L^{NO2}}$ $[N_2O_2]$ donor set and two *cis*-chloro ligands, therefore leading to a monoanionic species whose charge is balanced by a triethylammonium cation. $\mathbf{L^{R}Fe^{II}(Solv)_{x}}$ and $\mathbf{L^{R}Fe^{III}}$ chlorido complexes were also characterized in solution by UV-visible (Figure 1B and Table S3) and Mössbauer (Figure S9 and Table S3) spectroscopies, and electrochemistry (Table S3). The Mössbauer spectra of ferrous compounds, recorded in solution at 80 K, all appear as a quadrupole doublet. They could be simulated with isomer shifts close to 1.15 mm s^{-1} and a quadrupole splitting in the range 2.0 - 3.3 mm s^{-1} which are indicative of high spin S=2 ions.

The catalytic efficiencies of the four complexes were evaluated at 25 °C in conditions identical to the mild ones used in our previous report (Table 1).[14] In particular acetonitrile was selected as solvent for increased catalyst solubility and higher conversion. The yields obtained after 8 h reaction indicate that aziridination by mononuclear complexes $\mathbf{L^{R}Fe^{II}(NCMe)_2}$ is favored by the electron withdrawing groups of the ligand R = *t*Bu (5 %) < Cl (17 %) < NO_2 (31 %). But they are largely outweighed by the binuclear catalyst **(1)** (89 %). Conversely we found that aziridination is favored by electrodonating substituents on styrene. Indeed competitive aziridinations run with $\mathbf{L^{NO2}Fe^{II}(NCMe)_2}$ showed a yield (Y_X) increase from *p*-CN to *p*-OMe (Table S7). Moreover the log(Y_X/Y_H) data could be linearly correlated to the σ^+ parameter accounting for inductive and resonance effects of substituents (Figure S11). A moderately negative value of the slope (ρ^+ = -0.38) of the correlation indicates an electrophilic active species (see below) and a partial charge transfer in the transition state consistent with our previous studies of $\mathbf{H_2L^{Cl}}$ ligand.[14]

Table 1. Catalytic aziridination of styrene[a] and catalysts properties.

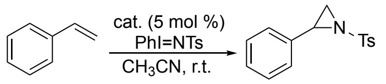

Precatalyst $\mathbf{L^{R}Fe^{II}(NCCH_3)_2}$	$\mathbf{L^{\mathit{t}Bu}}$	$\mathbf{L^{Cl}}$	$\mathbf{L^{NO2}}$	**(1)**
Aziridination yield[b] (%)	5	17	31	89
EA of $\mathbf{L^{R}Fe^{III}\text{-}{}^{\bullet}NTs}$[c]	110	124	127	143
E(Fe^{III}/Fe^{II}) of $\mathbf{L^{R}Fe^{III}}$ chlorides[d]	-0.89	-0.64	-0.34	

[a] Reaction conditions: Catalyst/PhI=NTs/styrene molar ratio 0.05/1/10, CH_3CN, 25 °C. [b] Yield (±3 % vs PhI=NTs) determined by ^{1}H-NMR spectroscopy of crude reaction mixtures using mesitylene as internal standard. No aziridine is formed in absence of catalyst. [c] DFT calculated values in kcal mol^{-1} (Table S11). [d] in V vs Ag/$AgNO_3$ (0.01 M) in CH_3CN + 0.1 M TBAP.

To substantiate this observation, we pursued DFT calculations. Considering the previous studies on NTs

10.1002/cctc.201901211

transfer with Fe complexes,[8,9,14,37] we focused our modelling on the Fe^{IV}-imido active species. As a matter of fact we investigated their main molecular and thermodynamics features when changing the substituent from *t*Bu to Cl to NO_2. Geometry optimizations of the three active species in quintet spin state (see SI) yielded very similar structures with the three ligands (Figures 2 and S12 and Table S8).

Based on spin densities on Fe and NTs group (Table S8), the electronic configuration is consistent with an Fe^{III}-$^{\bullet}$NTs radical species rather than an Fe^{IV}=NTs complex. A similar situation has been already observed in such high-valent Fe imido complexes.[8,9,14,38,39] The Fe-NTs distances in the three complexes are close to 1.9 Å, similarly to previous studies of high spin Fe^{III}-$^{\bullet}$NTs.[14,38] The EA were calculated for the three active species. They are fully consistent with the expected increase in electrophilicity from the *t*Bu substituent to the Cl and the nitro one (EA = 109.5, 123.7 and 126.3 kcal mol^{-1}, respectively, see Table S9 for details). It is worth noting that this matches perfectly the trend revealed by catalytic studies.

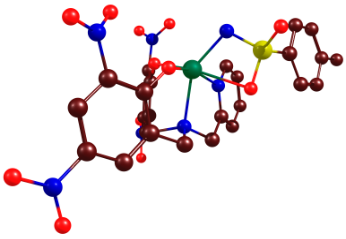

Figure 2. Optimized geometries (B3LYP-D3/BS1) of **$L^{NO2}Fe^{III}$-$^{\bullet}$NTs**. The two phenol groups are oriented in front and on the left and the pyridine ligand in the back. The H atoms are omitted for sake of simplicity.

To strengthen this apparent correlation between EA of catalyst and aziridination efficacy, we investigated the electrochemical properties of **$L^{R}Fe^{III}$** chlorido complexes, the oxidized counterparts of the Fe^{II} precursors. All of them present at least a one-electron reductive process (Figure 1C and S10) in the 0 to -0.9 V range in CH_3CN electrolyte solution, in addition to two ligand-centered oxidation processes (Figure S10). As already proposed for similar Fe^{III} complexes,[28,40] we assigned the reductive process to the $Fe^{III/II}$ one-electron reduction process. This assignment was confirmed by performing exhaustive electrolyses at applied $Fe^{III/II}$ reduction potentials. Strong differences in the shapes of the cyclic voltammograms and in the values of the reduction potential (Figure 1C) of **$L^{R}Fe^{III}$** chlorido complexes were observed. They illustrate clearly the major influence of the substitution of the phenolate ligand on the Fe electronic properties.

The CV of **$L^{tBu}Fe^{III}Cl$** complex (Figure 1C (a)) exhibits an irreversible redox system, with a reduction peak at E_{pc} = -0.89 V associated with an oxidation peak at E_{pa} = -0.38 V on the reverse scan. This behavior indicates that the one-electron reduction is associated to a chemical change which was assigned to the release of chloride ions. The presence of Cl^- in electrolyte solution was indeed evidenced by detection of its oxidation peak after performing a one-electron exhaustive reduction at -0.97 V.

When diphenolates are substituted by four chlorines (**H_2L^{Cl}**), which have a moderate electron withdrawing character, the **$[L^{Cl}Fe^{III}Cl_2]^-$** complex exhibits a quasi-reversible behavior (E_{pc} = -0.64 V, E_{pa} = -0.47 V, ΔE_p = 0.17 V, Figure 1C (b)). As for the above **$L^{tBu}Fe^{III}Cl$**, chlorides are released during the exhaustive one-electron reduction of the solution. Finally, the **$[L^{NO2}Fe^{III}Cl_2]^-$** complex exhibits two close reversible reduction peaks at $E_{1/2}$ = -0.34 and -0.57 V (Figure 1C (c)). CV investigations with varying scan rates suggested that these two systems correspond to two Fe^{III} species of very close structure which are not in equilibrium. This result is consistent with Mössbauer spectroscopy which showed two Fe^{III} species for **$[L^{NO2}Fe^{III}Cl_2]^-$** but a single species for **$L^{NO2}Fe^{II}(Py)_2$** (Figure S9). We have assigned the $Fe^{III/II}$ reversible system at the less negative potential, to **$[L^{NO2}Fe^{III}Cl_2]^-$** complex.[41,42] In conclusion, this cyclic voltammetry study illustrates the strong influence of ligand substitution on the electronic properties of the complexes.

To our delight, we observed also that the variation of the catalytic efficiencies parallels the evolution of the $Fe^{III/II}$ reduction potential of **$L^{R}Fe^{III}$** chlorido complexes (Figure 3). A similar effect was observed recently for Mn^{II} catalysts.[23] This finding highlights how ligand substitution tunes Fe electronic properties and hence the overall activity of the catalyst.

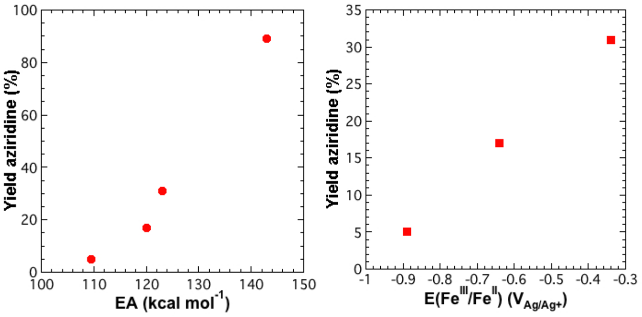

Figure 3. Correlation of the aziridination yield with (left) the electron affinity of the purport **$L^{R}Fe^{III}$** chlorido complexes.

This combined experimental and theoretical study thus confirms our initial finding that EA of the active species plays a major role on styrene aziridination by this family of Fe phenolate complexes. Moreover, it shows that there is a monotonous trend between EA and the aziridination yield (Figure 3) which extends over a large EA range (> 30 kcal mol^{-1}). In addition, a similar trend links aziridination yields to the $Fe^{III/II}$ reduction potential of the catalyst precursor (Figure 3). This illustrates that the aziridination capacity of the catalyst (i) reflects the intrinsic electronic properties of the system and (ii) can be evaluated by cyclic voltammetry experiments.

In addition, this study was made possible by the introduction of a new ligand **H_2L^{NO2}** with four nitro substituents. The influence of these substituents manifests in solid state and solution properties of the ligand and its Fe complexes. We showed here that this substitution eventually led to a substantial enhancement in catalytic performance for olefin aziridination. The same kind of activity enhancement can be anticipated for acidic catalysis involving Fe or other metals.[34,43]

Experimental Section

Experimental details are provided as supplementary information.

Acknowledgements

S. C.-N., P. M. and J.-M. L. thank the Labex ARCANE and CBH-EUR-GS (ANR-17-EURE-0003) for partial funding. This work was performed using HPC resources from GENCI-CINES (Grant 2016-c2016087 648) and GENCI-IDRIS (Grant 2017-A0020807648).

Conflict of interest

The authors declare no conflict of interest.

Keywords: aziridination • iron catalyst • DFT calculations • redox properties • mechanism

[1] H. M. L. Davies, J. R. Manning, *Nature* **2008**, *451*, 417–424.
[2] J. Roizen, M. Harvey, J. DuBois, *Acc. Chem. Res.* **2012**, *45*, 911–922.
[3] L. Maestre, W. M. C. Sameera, M. Mar Diaz-Requejo, F. Maseras, P. J. Pérez, *J. Am. Chem. Soc.* **2013**, *135*, 1338–1348.
[4] V. Bagchi, P. Paraskevopoulou, P. Das, L. Chi, Q. Wang, A. Choudhury, J. S. Mathieson, L. Cronin, D. B. Pardue, T. R. Cundari, et al., *J. Am. Chem. Soc.* **2014**, *136*, 11362–11381.
[5] L.-M. Jin, X. Xu, H. Lu, X. Cui, L. Wojtas, X. P. Zhang, *Angew. Chem. Int. Ed. Engl.* **2013**, *52*, 5309–5313.
[6] P. K. Kuijpers, J. I. van der Vlugt, P. Schneider, B. de Bruin, *Chem. Eur. J.* **2017**, *23*, 13819–13829.
[7] S. M. Paradine, M. C. White, *J. Am. Chem. Soc.* **2012**, *134*, 2036–2039.
[8] S. Kumar, A. S. Faponle, P. Barman, A. K. Vardhaman, C. V. Sastri, D. Kumar, S. P. de Visser, *J. Am. Chem. Soc.* **2014**, *136*, 17102–17115.
[9] S. Hong, X. Lu, Y.-M. Lee, M. S. Seo, T. Ohta, T. Ogura, M. Clémancey, P. Maldivi, J.-M. Latour, R. Sarangi, et al., *J. Am. Chem. Soc.* **2017**, *139*, 14372–14375.
[10] R. E. Cowley, N. A. Eckert, S. Vaddadi, T. M. Figg, T. R. Cundari, P. L. Holland, *J. Am. Chem. Soc.* **2011**, *133*, 9796–9811.
[11] M. J. T. Wilding, D. A. Iovan, A. T. Wrobel, J. T. Lukens, S. N. MacMillan, K. M. Lancaster, T. A. Betley, *J. Am. Chem. Soc.* **2017**, *139*, 14757–14766.
[12] A. Fingerhut, O. V. Serdyuk, S. B. Tsogoeva, *Green Chem.* **2015**, *17*, 2042–2058.
[13] C. Damiano, D. Intrieri, E. Gallo, *Inorganica Chim. Acta* **2018**, *470*, 51–67.
[14] R. Patra, G. Coin, L. Castro, P. Dubourdeaux, M. Clémancey, J. Pécaut, C. Lebrun, P. Maldivi, J.-M. Latour, *Catal. Sci. Technol.* **2017**, *7*, 4388–4400.
[15] D. W. Crandell, S. B. Munoz III, J. M. Smith, M.-H. Baik, *Chem. Sci.* **2018**, *9*, 8542–8552.
[16] S. B. Isbill, P. P. Chandrachud, J. L. Kern, D. M. Jenkins, S. Roy, *ACS Catal.* **2019**, *9*, 6223–6233.
[17] J. P. Mahy, G. Bedi, P. Battioni, D. Mansuy, *J. Chem. Soc. Perkin Trans. 2* **1988**, 1517–1524.
[18] Y. Liu, C.-M. Che, *Chem. Eur. J.* **2010**, *16*, 10494–10501.
[19] E. T. Hennessy, R. Y. Liu, D. A. Iovan, R. A. Duncan, T. A. Betley, *Chem. Sci.* **2014**, *5*, 1526–1532.
[20] P. P. Chandrachud, H. M. Bass, D. M. Jenkins, *Organometallics* **2016**, *35*, 1652–1657.
[21] P. Liu, E. L.-M. Wong, A. W.-H. Yuen, C.-M. Che, *Org. Lett.* **2008**, *10*, 3275–3278.
[22] M. F. Shehata, S. K. Ayer, J. L. Roizen, *J. Org. Chem.* **2018**, *83*, 5072–5081.
[23] V. Bagchi, A. Kalra, P. Das, P. Paraskevopoulou, S. Gorla, L. Ai, Q. Wang, S. Mohapatra, A. Choudhury, Z. Sun, et al., *ACS Catal.* **2018**, *8*, 9183–9206.
[24] C. M. Anderson, A. M. Aboelenen, M. P. Jensen, *Inorg. Chem.* **2019**, *58*, 1107–1119.
[25] A. C. Mayer, A.-F. Salit, C. Bolm, *Chem. Commun.* **2008**, 5975–5977.
[26] F. Avenier, J.-M. Latour, *Chem. Commun.* **2004**, 1544–1545.
[27] E. Gouré, F. Avenier, P. Dubourdeaux, O. Sénèque, F. Albrieux, C. Lebrun, M. Clémancey, P. Maldivi, J.-M. Latour, *Angew. Chem. Int. Ed.* **2014**, *53*, 1580–1584.
[28] R. Viswanathan, M. Palaniandavar, T. Balasubramanian, T. Muthiah, *Inorg. Chem.* **1998**, *37*, 2943–2951.
[29] S. Heidari, E. Safaei, A. Wojtczak, P. Cotic, A. Kozakiewicz, *Polyhedron* **2013**, *55*, 109–116.
[30] J. Farrell, J. A. Niconchuk, P. R. Renehan, C. S. Higham, E. Yoon, M. V. Andrews, J. L. Shaw, A. Cetin, J. Engle, C. J. Ziegler, *Dalton Trans.* **2014**, *43*, 6610–6613.
[31] A. M. Reckling, D. Martin, L. N. Dawe, A. Decken, C. M. Kozak, *J. Organomet. Chem.* **2011**, *696*, 787–794.
[32] L. E. N. Allan, J. P. MacDonald, G. S. Nichol, M. P. Shaver, *Macromolecules* **2014**, *47*, 1249–1257.
[33] H. Schroeder, B. R. M. Lake, S. Demeshko, M. P. Shaver, M. Buback, *Macromolecules* **2015**, *48*, 4329–4338.
[34] M. Taherimehr, J. P. Cardoso Costa Serta, A. W. Kleij, C. J. Whiteoak, P. P. Pescarmona, *ChemSusChem* **2015**, *8*, 1034–1042.
[35] K. Zhu, M. P. Shaver, S. P. Thomas, *Chem. Asian J.* **2016**, *11*, 977–980.
[36] K. Zhu, M. P. Shaver, S. P. Thomas, *Chem. Sci.* **2016**, *7*, 3031–3035.
[37] E. J. Klinker, T. A. Jackson, M. P. Jensen, A. Stubna, G. Juhász, E. L. Bominaar, E. Münck, L. Que, *Angew. Chem. Int. Ed.* **2006**, *45*, 7394–7397.
[38] E. R. King, E. T. Hennessy, T. A. Betley, *J. Am. Chem. Soc.* **2011**, *133*, 4917–4923.
[39] M. Jaccob, G. Rajaraman, *Dalton Trans.* **2012**, *41*, 10430–10439.
[40] R. K. Dean, C. I. Fowler, K. Hasan, K. Kerman, P. Kwong, S. Trudel, D. B. Leznoff, H.-B. Kraatz, L. N. Dawe, C. M. Kozak, *Dalton Trans.* **2012**, *41*, 4806–4816.
[41] **n.d.**
[42] K. Ambrose, K. N. Robertson, C. M. Kozak, *Dalton Trans.* **2019**, *48*, 6248–6260.
[43] K. A. Andrea, T. R. Brown, J. N. Murphy, D. Jagota, D. McKearney, C. M. Kozak, F. M. Kerton, *Inorg. Chem.* **2018**, *57*, 13494–13504.

10.1002/cctc.201901211

Entry for the Table of Contents

Layout 1:

COMMUNICATION

Iron aminophenolates: aziridination yields parallel the $Fe^{III/II}$ reduction potentials of the catalyst precursors allowing to evaluate the aziridination capacity of the catalyst by cyclic voltammetry experiments.

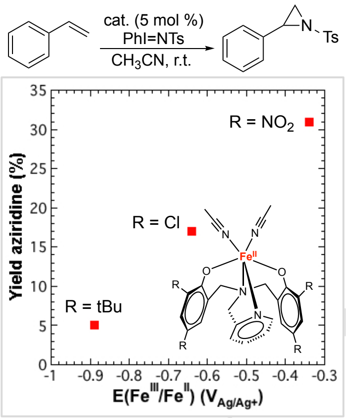

Dr. Guillaume Coin, Dr. Ranjan Patra, Dr. Martin Clémancey, Dr. Jacques Pécaut, Colette Lebrun, Dr. Ludovic Castro, Dr. Pascale Maldivi, Dr. Sylvie Chardon-Noblat, Dr. Jean-Marc Latour**

Page No. – Page No.

Fe-based complexes as styrene aziridination catalysts: ligand substitution tunes catalyst activity